

Supplementary material

Modelling of secondary organic aerosol formation from isoprene photooxidation chamber studies using different approaches

Haofei Zhang,^{A,B,C} Harshal M. Parikh,^A Jyoti Bapat,^A Ying-Hsuan Lin,^A Jason D. Surratt^A and Richard M. Kamens^A

^ADepartment of Environmental Sciences and Engineering, Gillings School of Global Public Health, The University of North Carolina at Chapel Hill, Chapel Hill, NC 27599, USA.

^BPresent address: Lawrence Berkeley National Laboratory, Berkeley, CA 94720, USA.

^CCorresponding author. Email: hfzhang@lbl.gov

Mathematical details of the dynamic gas-particle partitioning theory

A dynamic gas-particle partitioning approach was previously described in Bowman et al.^[1] and Koo et al.^[2] In general, the total change in particle-phase mass concentration of semi-volatile product i is obtained by combining the flux equation that determines the transport of i from gas to particle phase (Eqn S1) (Seinfeld and Pandis^[3]) and the particle number concentration for each particle-size section:

$$\frac{dc_{a,i,k}}{dt} = \frac{2\pi N_k d_{p,k} D_i}{2\lambda / ad_{p,k} + 1} \left(c_{g,i} - x_{i,k} c_{sat,i}^* \exp\left(\frac{4\sigma_i v_i}{RTd_{p,k}}\right) \right) \quad (S1)$$

where N_k (m^{-3}) and $d_{p,k}$ (m) are the number concentration and mean diameter of particles in size-bin section k , D_i ($\text{m}^2 \text{s}^{-1}$) is the gas-phase diffusivity of i , λ (m) is the mean free path of air, a is the gas-particle accommodation coefficient, $c_{a,i,k}$ ($\mu\text{g m}^{-3}$) is the aerosol-phase concentration of i in particle size-section k , $c_{g,i}$ ($\mu\text{g m}^{-3}$) is the bulk gas-phase concentration of i and $x_{i,k}$ is the mole fraction of i in the aerosol phase for size section k . The exponential term in Eqn S1 represents the Kelvin effect correction for the equilibrium concentration of i at the particle surface, where σ_i (N m^{-1}) is the surface tension of i and v_i ($\text{m}^3 \text{mol}^{-1}$) is the molar volume of i . $c_{sat,i}^*$ ($\mu\text{g m}^{-3}$) is the saturation concentration of semi-volatile product i at a particular temperature T . The temperature dependence of saturation concentration is calculated using Clausius–Clapeyron equation:

$$c_{sat,i}^* = c_{sat,i(ref)}^* \frac{T_{ref}}{T} \exp\left[\frac{\Delta H_{vap}}{R} \left(\frac{1}{T_{ref}} - \frac{1}{T}\right)\right] \quad (S2)$$

where $c_{sat,i(ref)}^*$ ($\mu\text{g m}^{-3}$) is the saturation concentration of product i at reference temperature T_{ref} (K), ΔH_{vap} (kJ mol^{-1}) is the enthalpy of vaporisation and R is the universal gas constant. $c_{sat,i(ref)}^*$

values are either obtained using curve-fitting to experimental yield data for Odum-type two-product parameterisations (Odum et al.^[4]) or are assumed to represent volatility bins that are regularly spaced by factors of 10 in c^* -space for VBS approach (Donahue et al.^[5]).

The change in bulk gas-phase concentration of i is:

$$\frac{dc_{g,i}}{dt} = P_i - \sum_k \frac{dc_{a,i,k}}{dt} \quad (\text{S3})$$

where P_i ($\mu\text{g m}^{-3} \text{ s}^{-1}$) is the rate of production of i from chemical reaction.

The dynamic partitioning approach determines the particle phase concentration for $(m + n)$ semi-volatile products in every particle size-section k , using the full dynamic approach described in Eqns S1 and S2 by solving an ordinary differential equation system comprising $(m + n) \times k + 1$ number of equations.

In the event of particle size and number distribution data being available (as for this paper) or computed using an presumed particle size distribution at every timestep, numerous assumptions can be made to simplify the fully dynamic approach: (1) mole fraction of a product i in aerosol phase is independent of particle size, i.e. $x_i = x_{i,k}$; (2) the aerosol chemical composition changes slowly during a timestep. For the purposes of mole fraction calculation of i , ca, it $c_{a,i}^t \approx c_{a,i}^{t-\Delta t}$, where t is the current solution time and Δt is the previous timestep. These two assumptions lead to:

$$\frac{dc_{g,i}}{dt} P_i - D_i \left[\sum_k \frac{2\pi N_k d_{p,k}}{2\lambda} c_{g,i} - \frac{\frac{c_{a,i}^{t-\Delta t}}{M_i}}{\frac{C_0}{M_0} + \sum_{j=1}^{m+n} \frac{c_{a,j}^{t-\Delta t}}{M_j}} \times c_{sat,i}^* \sum_k \frac{2\pi N_k d_{p,k}}{\frac{2\lambda}{ad_{p,k}} + 1} \exp\left(\frac{4\sigma_i v_i}{RTd_{p,k}}\right) \right] \quad (\text{S4})$$

where N_k (m^{-3}) and $d_{p,k}$ (m) are the number concentration and mean diameter of particles in size-bin section k , D_i ($\text{m}^2 \text{ s}^{-1}$) is the gas-phase diffusivity of i , λ (m) is the mean free path of air, a is the gas-particle accommodation coefficient, $c_{a,i,k}$ ($\mu\text{g m}^{-3}$) is the particle-phase concentration of i in the particle size-section k , $c_{g,i}$ ($\mu\text{g m}^{-3}$) is the bulk gas-phase concentration of i , $x_{i,k}$ is the mole fraction of i in the particle phase for size section k , σ_i (N m^{-1}) is the surface tension of i , v_i ($\text{m}^3 \text{ mol}^{-1}$) is the molar volume of i and P_i ($\mu\text{g m}^{-3} \text{ s}^{-1}$) is the rate of production of i from chemical reactions. P_i can be obtained using semi-volatile product formation equations for high-NO and low-NO pathways (Eqns S5, S6) and Eqn S4 can be solved to compute bulk gas-phase

concentrations of each semi-volatile product i using either explicit or multistep numerical methods.

$$c_{tot,i,high} = c_{gas,i,high} + c_{part,i,high} = \frac{\alpha_{i,high}}{\alpha_{i,tot}} \times ISOPHRXN \quad (S5)$$

$$c_{tot,i,low} = c_{gas,i,low} + c_{part,i,low} = \frac{\alpha_{i,low}}{\alpha_{i,tot}} \times ISOPLRXN \quad (S6)$$

where $c_{tot,i,high}$ ($\mu\text{g m}^{-3}$) is the total concentration of the empirical semi-volatile product i from high-NO pathway (in gas and aerosol phase, $c_{gas,i,high} + c_{part,i,high}$) and $c_{tot,i,low}$ ($\mu\text{g m}^{-3}$) is the total concentration of the empirical semi-volatile product i (in gas and aerosol phase, $c_{gas,i,low} + c_{part,i,low}$) from low-NO pathway. $\Delta ISOPHRXN$ and $\Delta ISOPLRXN$ are the corresponding change in counter species used to track the contribution via reactions under high- and low-NO conditions ($\mu\text{g m}^{-3}$). $\alpha_{i,high}$ in Eqn S5 and $\alpha_{i,low}$ in Eqn S6 represent the stoichiometric product coefficients determined in previous studies by fitting high-NO and low-NO chamber data to a parameterised yield curve.

From the bulk gas-phase concentration of i , the particle-phase concentration at solution t is:

$$c_{a,i}^t = c_{tot,i}^t - c_{g,i}^t \quad (S7)$$

Estimate of aerosol aqueous-phase acidity and uncertainties

In the aerosol aqueous-phase, the acidity is estimated based upon the concentrations of NH_4^+ , SO_4^{2-} and NO_3^- in the aqueous phase. Initial NH_4^+ and SO_4^{2-} data are available in the experiments and their decay rates can be estimated according to seed decay rate. Gas-phase HNO_3 concentrations with time are modelled using the gas-phase mechanism (ISO-UNC). Thus the NO_3^- in the aqueous phase is calculated based on the Henry's Law constant of HNO_3 ($2.1 \times 10^5 \text{ M atm}^{-1}$, which has some uncertainties).

The free H^+ can be written base on charge balance as:

$$[\text{H}^+] = 2 [\text{SO}_4^{2-}] - [\text{NH}_4^+] + [\text{NO}_3^-] \quad (S8)$$

However, as the SOA forms, some SO_4^{2-} ions are converted from inorganic ions to organosulfate. Thus:

$$[\text{H}^+] = 2 ([\text{SO}_4^{2-}] - [\text{Organosulfate}]) - [\text{NH}_4^+] + [\text{NO}_3^-] \quad (S9)$$

Here, assuming the conversion of SO_4^{2-} to organosulfate is negligible, the online version of the extended aerosol thermodynamics model (E-AIM II: $\text{H}^+ - \text{NH}_4^+ - \text{SO}_4^{2-} - \text{NO}_3^- - \text{H}_2\text{O}$) was used to estimate aerosol acidity. Modelling outputs of activity coefficient and moles of H^+_{aq} in the

aqueous phase, and the total volume of aqueous phase in the aerosol per cubic metre of air in the thermodynamic equilibrium were used to calculate aerosol pH.

$$\text{pH} = -\log [\gamma_{\text{H}^+}^{\text{aq}} \times n_{\text{H}^+}^{\text{aq}} \div (V_{\text{aq}} \div 1000)] \quad (\text{S10})$$

Table S1. Dynamic gas-particle partitioning parameters

2-Product model				
High NO _x				
<i>v_i</i> , Molar volume (m ³ mol ⁻¹)	1.65 × 10 ⁻⁴	1.36 × 10 ⁻⁴		
<i>D_i</i> , Diffusivity (m ² s ⁻¹)	6.21 × 10 ⁻⁶	6.75 × 10 ⁻⁶		
<i>σ_i</i> , Surface Tension (N m ⁻¹)	0.03	0.03		
Accommodation coefficient	0.0005	0.0005		
Low NO _x				
<i>v_i</i> , Molar volume (m ³ mol ⁻¹)	1.93 × 10 ⁻⁴			
<i>D_i</i> , Diffusivity (m ² s ⁻¹)	5.79 × 10 ⁻⁶			
<i>σ_i</i> , Surface Tension (N m ⁻¹)	0.03			
Accommodation coefficient	0.0005			
Volatility basis-set				
High NO _x				
<i>v_i</i> , Molar volume (m ³ mol ⁻¹)	1.65 × 10 ⁻⁴	1.55 × 10 ⁻⁴	1.46 × 10 ⁻⁴	1.36 × 10 ⁻⁴
<i>D_i</i> , Diffusivity (m ² s ⁻¹)	6.20 × 10 ⁻⁶	6.54 × 10 ⁻⁶	6.62 × 10 ⁻⁶	7.08 × 10 ⁻⁶
<i>σ_i</i> , Surface Tension (N m ⁻¹)	0.03	0.03	0.03	0.03
Accommodation coefficient	0.001	0.001	0.001	0.001
Low NO _x				
<i>v_i</i> , Molar volume (m ³ mol ⁻¹)	1.93 × 10 ⁻⁴	1.74 × 10 ⁻⁴	1.55 × 10 ⁻⁴	1.36 × 10 ⁻⁴
<i>D_i</i> , Diffusivity (m ² s ⁻¹)	5.77 × 10 ⁻⁶	6.21 × 10 ⁻⁶	6.44 × 10 ⁻⁶	7.08 × 10 ⁻⁶
<i>σ_i</i> , Surface Tension (N m ⁻¹)	0.03	0.03	0.03	0.03
Accommodation coefficient	0.001	0.001	0.001	0.001

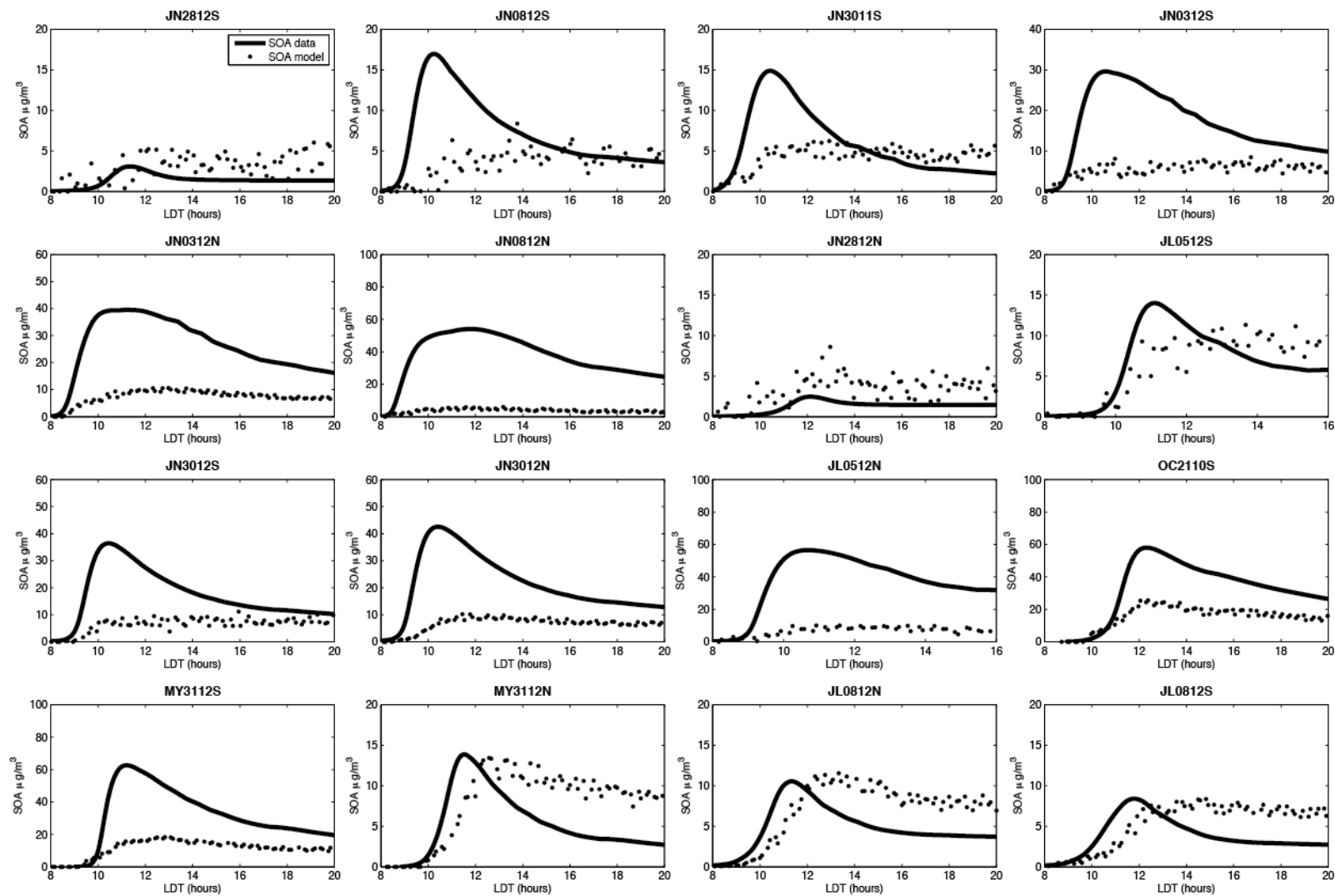


Fig. S1. Simulations of all the experiments using the VBS_{equilibrium} model. (LDT, local day time.)

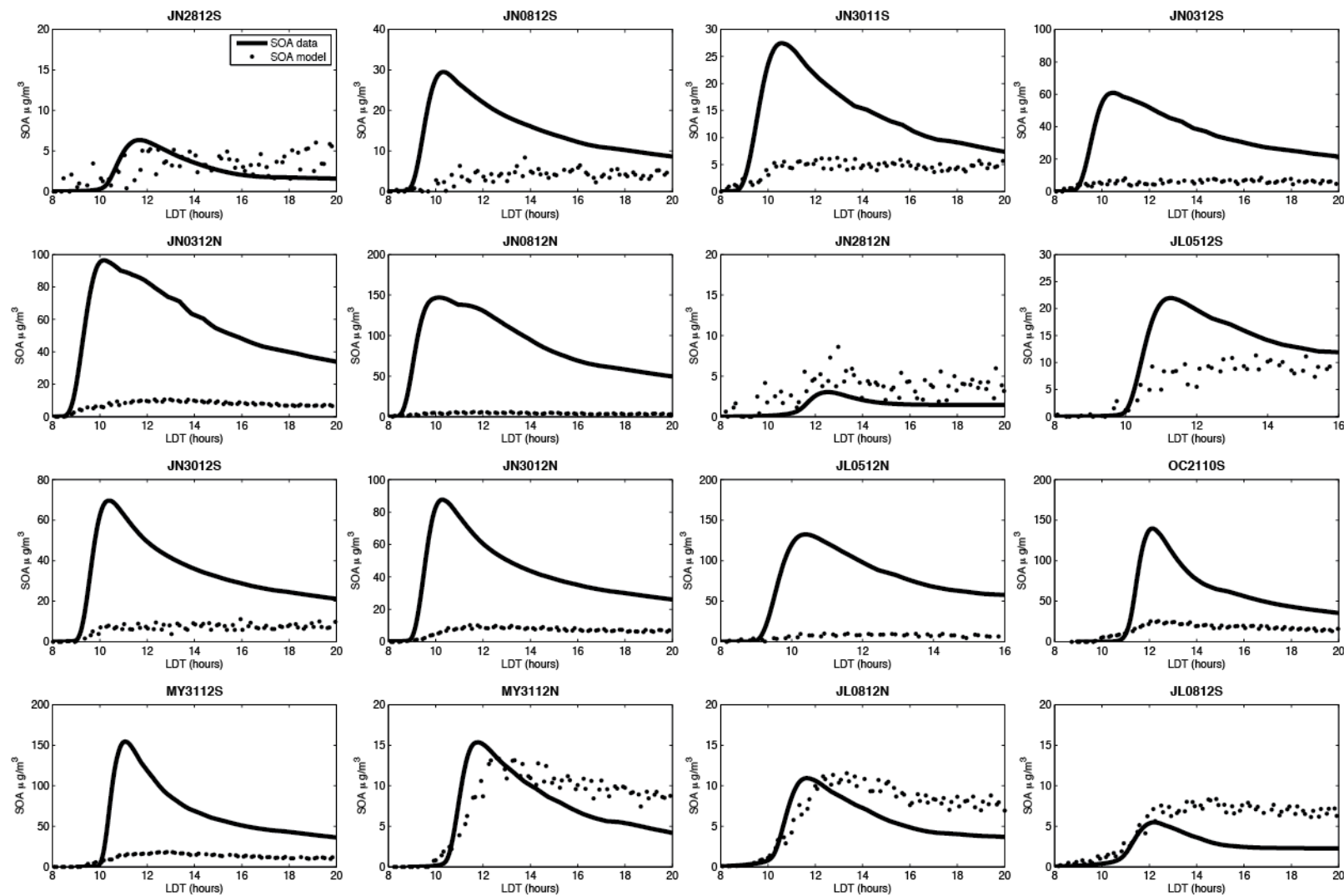


Fig. S2. Simulations of all the experiments using the Odum two-product_equilibrium model. (LDT, local day time.)

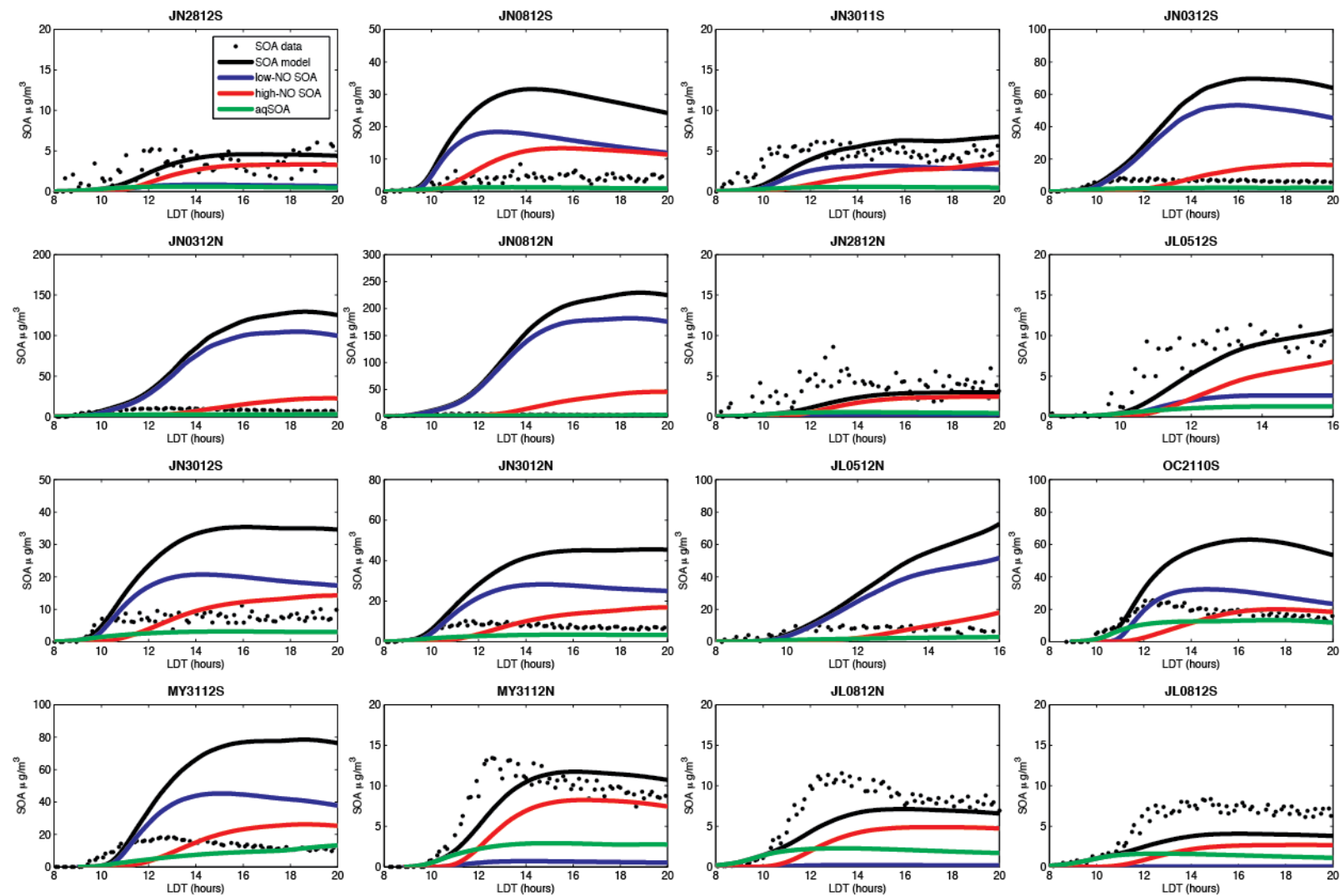


Fig. S3. Simulations of all the experiments using the kinetic_equilibrium model. (LDT, local day time.)

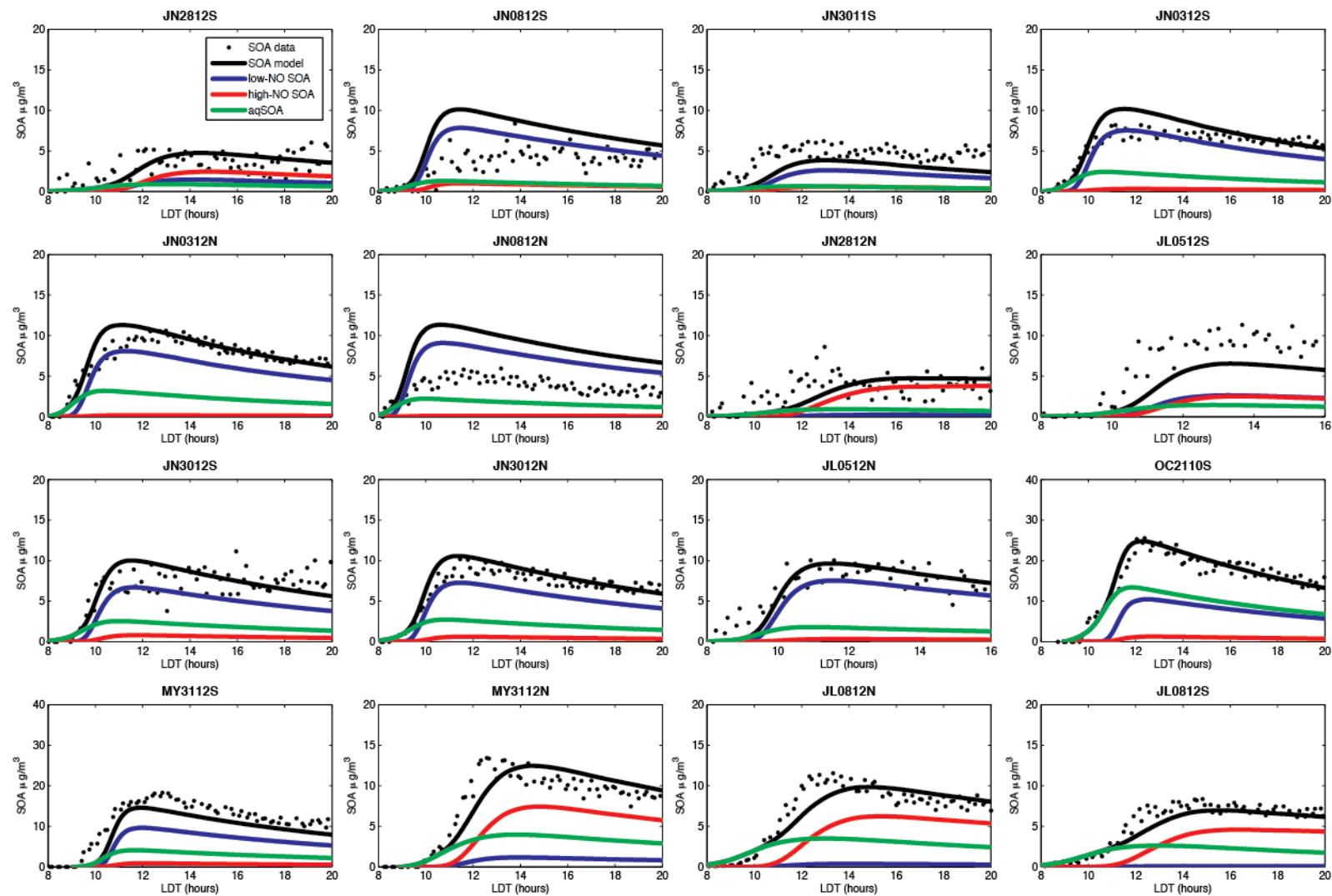


Fig. S4. Simulations of all the experiments using the kinetic_non-equilibrium model. (LDT, local day time.)

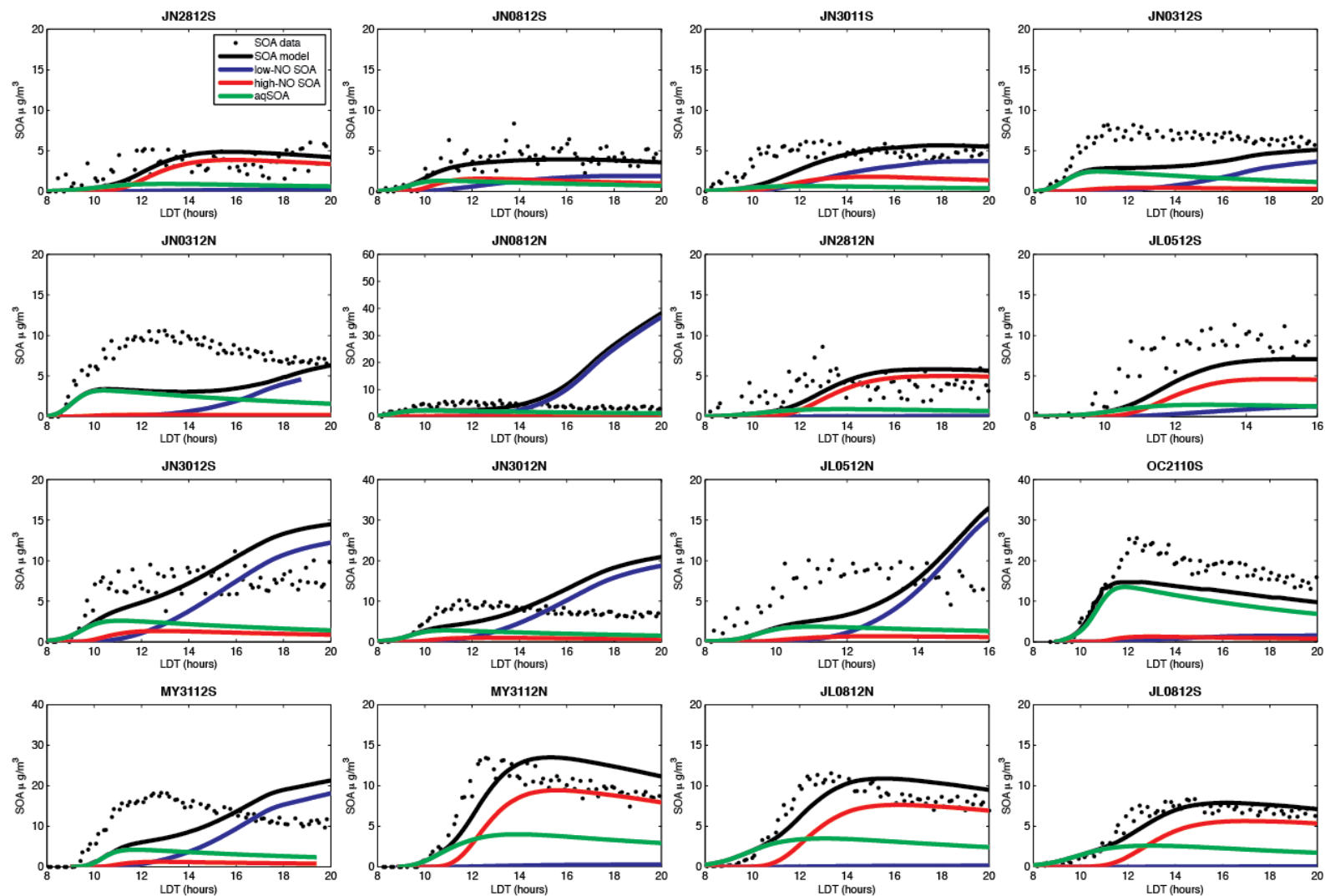


Fig. S5. Simulations of all the experiments using the IEPOX aqueous-phase model. (LDT, local day time.)

References

- [1] F. M. Bowman, J. R. Odum, J. H. Seinfeld, S. N. Pandis, Mathematical model for gas-particle partitioning of secondary organic aerosols. *Atmos. Environ.* **1997**, *31*, 3921. [doi:10.1016/S1352-2310\(97\)00245-8](https://doi.org/10.1016/S1352-2310(97)00245-8)
- [2] B. Y. Koo, A. S. Ansari, S. N. Pandis, Integrated approaches to modeling the organic and inorganic atmospheric aerosol components. *Atmos. Environ.* **2003**, *37*, 4757. [doi:10.1016/j.atmosenv.2003.08.016](https://doi.org/10.1016/j.atmosenv.2003.08.016)
- [3] J. H. Seinfeld, S. N. Pandis, *Atmospheric Chemistry and Physics: From Air Pollution to Climate Change* **1998** (Wiley: New York).
- [4] J. R. Odum, T. Hoffmann, F. M. Bowman, D. Collins, R. C. Flagan, J. H. Seinfeld, Gas/particle partitioning and secondary organic aerosol yields. *Environ. Sci. Technol.* **1996**, *30*, 2580. [doi:10.1021/es950943+](https://doi.org/10.1021/es950943+)
- [5] N. M. Donahue, A. L. Robinson, C. O. Stanier, S. N. Pandis, Coupled partitioning, dilution, and chemical aging of semivolatile organics. *Environ. Sci. Technol.* **2006**, *40*, 2635. [doi:10.1021/es052297c](https://doi.org/10.1021/es052297c)